Groh, R., & Pirrera, A. (2017). Exploring islands of stability in the design space of cylindrical shell structures. In W. Pietraszkiewicz, & W. Witkowski (Eds.), *Shell Structures: Theory and Applications Volume 4: Proceedings of the 11th International Conference "Shell Structures: Theory and Applications, (SSTA 2017), October 11-13, 2017, Gdansk, Poland* (pp. 223-226). Routledge.

Peer reviewed version

Link to publication record in Explore Bristol Research

PDF-document

Exploring islands of stability in the design space of cylindrical shell structures

R.M.J. Groh & A. Pirrera
Bristol Composites Institute (ACCIS)
Department of Aerospace Engineering
University of Bristol, Bristol, UK

ABSTRACT: The structural stability of a simple benchmark problem – the snap through of a shallow cylindrical roof – is revisited. The problem is analysed in a robust manner using a technique known as *generalised path-following*, which combines the mathematical domains of finite element analysis and numerical continuation. Using this technique, the well-known arc-length method for tracing equilibrium paths in load-displacement space is extended to explore other interesting paths on a two-dimensional solution manifold in three-dimensional load-displacement-parameter space. These paths include unconventional equilibrium paths traced by varying a model parameter, *e.g.* shell thickness, as well as critical paths that describe points where the tangential stiffness matrix is singular – that is where buckling, snap-through or other instabilities occur. For the chosen benchmark problem, a localised region of stable equilibrium exists on one of the unstable equilibrium branches. The evolution of this stable region with variations in shell thickness is explored by tracing the locus of critical limit points that separate the stable and unstable portions of the equilibrium curve. Hence, without resorting to computationally expensive parametric studies, we establish a two-dimensional manifold of stable equilibria in displacement-load-thickness space, which can be graphically interpreted as an *island of stability*.

1 INTRODUCTION

Structural instabilities are generally regarded as unwanted aberrations rather than beneficial design features. The adoption of structures that exploit structural nonlinearities, *e.g.* morphing composites that use snap-buckling as a shape-changing mechanism, has been hampered for a dearth of numerical methods to analyse these structures robustly and efficiently, particularly in a manner that is compatible with accepted methods used in industry. The importance of robust computational tools for designing the next generation of optimised, thin-walled structures is paramount, especially because confidence in computational tools can serve as an enabler for non-conventional designs.

For example, the shape-changing mechanism of composite morphing structures is typically governed by instabilities that allow the structures to snap between two different equilibrium configurations (Pirrera, Avitabile, & Weaver 2012). Commercial finite element packages can be used to analyse morphing structures, but most of the time, these analyses are rather *ad hoc*, because current commercial finite element packages are incapable of robustly predicting instabilities in detail. In fact, the analyst needs to be aware of possible instabilities and distinct stable configurations *a priori*, and then "coax" the algorithm to land on the required mode shape, using, for example, initial imperfections (Pirrera, Avitabile, & Weaver 2012).

In pure and applied mathematics, a rich literature on the so-called *numerical continuation* techniques exists that are used to explore the solution space of nonlinear ordinary or partial differential equations in terms of a set of arbitrary parameters that govern the intrinsic properties or external factors acting on the physical system. When coupled with the concepts developed in bifurcation theory, a numerical continuation algorithm is capable of tracing any nonlinear solution path, traverse and identify different instability points, and switch onto other solution branches if so required. Hence, such an algorithm, embedded within the finite element method, significantly enhances the engineer's capability to design nonlinear structures.

The purpose of this paper is to showcase the capabilities of such a technique by means of a recurring benchmark problem that, to the authors' knowledge, has not been analysed to the extent presented here. We show that the design space of a cylindrical roof structure subjected to a transverse snap-through load contains a multitude of symmetry-breaking bifurcation branches, one of which, previously shown by Zhou *et*

al. (Zhou, Stanciulescu, Eason, & Spottswood 2015), displays a localised region of stability surrounded by unstable branches. Using the capabilities of the numerical continuation solver, we easily determine the bounds of this island of stability with respect to other parameters, in this case, the shell thickness.

2 THEORY

Path-following techniques in commercial finite element packages are based on tracing an equilibrium solution in two-dimensional load-displacement space. Such an equilibrium path only represents a single locus of points on a multi-dimensional solution manifold parametrised by any number of other variables such as material properties, geometric dimensions, *etc*. Therefore, conventional path-following methods are a specific subset of a generalised path-following technique which enables visualisation of the structural behaviour in multi-dimensional space (Eriksson 1997).

The conventional equilibrium of internal and external forces can be expressed as a function of a loading parameter, λ, and the displacement state variables, $\boldsymbol{u}$, in the form:

$$\boldsymbol{F}(\boldsymbol{u}, \lambda) = \boldsymbol{f}(\boldsymbol{u}) - \boldsymbol{p}(\lambda), \tag{1}$$

where $\boldsymbol{p}(\lambda)$ is the external (non-follower) load vector and $\boldsymbol{f}(\boldsymbol{u})$ is the internal force vector. For generalised path-following, Eq. (1) is adapted to incorporate any number of additional parameters, such that,

$$\boldsymbol{F}(\boldsymbol{u}, \boldsymbol{\Lambda}) = \boldsymbol{f}(\boldsymbol{u}, \boldsymbol{\Lambda}_1) - \boldsymbol{p}(\boldsymbol{\Lambda}_2), \tag{2}$$

where $\boldsymbol{\Lambda} = [\boldsymbol{\Lambda}_1^\top, \boldsymbol{\Lambda}_2^\top]^\top = [\lambda_1, \ldots, \lambda_p]^\top$ is a vector containing p control variables.

The n number of equilibrium equations in Eq. (2), correspond directly to the n number of displacement degrees of freedom in the system. Because the structural response is parametrised by p additional parameters, a p-dimensional solution manifold in $\mathbb{R}^{(n+p)}$ exists. Following the notation and framework by Eriksson (Eriksson 1997), specific solution subsets on the p-dimensional manifold are defined by incorporating additional auxiliary equations, $\boldsymbol{g}$. Hence, we wish to evaluate solutions to the augmented system

$$\boldsymbol{G}(\boldsymbol{u}, \boldsymbol{\Lambda}) \equiv \begin{pmatrix} \boldsymbol{F}(\boldsymbol{u}, \boldsymbol{\Lambda}) \\ \boldsymbol{g}(\boldsymbol{u}, \boldsymbol{\Lambda}) \end{pmatrix} = \boldsymbol{0}. \tag{3}$$

For r auxiliary equations, the solution to Eq. (3) becomes $(p-r)$-dimensional and hence $p-1$ auxiliary equations are required to define a one-dimensional curve, or so-called *subset curve* of the multi-dimensional solution manifold. As outlined by Eriksson (Eriksson 1997), these subset equations can define fundamental equilibrium paths (the fundamental load parameter is varied); parametric equilibrium paths (a non-load parameter is varied); bifurcation branches emanating from another equilibrium path; critical paths (the tangential stiffness matrix is singular); *etc*. To constrain the system to a locus of singular points, we need to simultaneously enforce the fulfillment of a criticality condition, *e.g.* $\boldsymbol{K}_T\boldsymbol{\phi} = \boldsymbol{0}$. In the most general form, q number of auxiliary variables $\boldsymbol{v}$ are added to the auxiliary equations $\boldsymbol{g}$,

$$\boldsymbol{G}(\boldsymbol{u}, \boldsymbol{\Lambda}, \boldsymbol{v}) \equiv \begin{pmatrix} \boldsymbol{F}(\boldsymbol{u}, \boldsymbol{\Lambda}) \\ \boldsymbol{g}(\boldsymbol{u}, \boldsymbol{\Lambda}, \boldsymbol{v}) \end{pmatrix} = \boldsymbol{0}. \tag{4}$$

Following the example from above, when the n-dimensional null vector at the critical state is introduced as the auxiliary variable, $\boldsymbol{v}$, a singular subset curve in two parameters, $p = 2$, is appropriately constrained by the associated $r = n + 1$ auxiliary equations $\boldsymbol{K}_T\boldsymbol{v} = \boldsymbol{0}$ and $||\boldsymbol{v}||_2 = 1$.

When evaluating one-dimensional curves ($r = p + q - 1$), one additional equation is needed to uniquely constrain the system to a solution point $\boldsymbol{y} = (\boldsymbol{u}, \boldsymbol{\Lambda}, \boldsymbol{v})$. Hence,

$$\boldsymbol{G}^N(\boldsymbol{y}) \equiv \begin{pmatrix} \boldsymbol{F}(\boldsymbol{u}, \boldsymbol{\Lambda}) \\ \boldsymbol{g}(\boldsymbol{u}, \boldsymbol{\Lambda}, \boldsymbol{v}) \\ N(\boldsymbol{u}, \boldsymbol{\Lambda}) \end{pmatrix} = \boldsymbol{0}, \tag{5}$$

where N is a scalar equation which plays the role of a multi-dimensional arc-length constraint. A specific solution to Eq. (5) is determined by a consistent linearisation coupled with a Newton-Raphson algorithm,

$$\boldsymbol{y}_{j+1} = \boldsymbol{y}_j - \left(\boldsymbol{G}^N_{,\boldsymbol{y}}(\boldsymbol{y}_j)\right)^{-1} \cdot \boldsymbol{G}^N(\boldsymbol{y}_j) \tag{6}$$

with

$$\boldsymbol{G}^N_{,\boldsymbol{y}} = \begin{bmatrix} \boldsymbol{F}_{,\boldsymbol{u}} & \boldsymbol{F}_{,\boldsymbol{\Lambda}} & \boldsymbol{0}_{n\times q} \\ \boldsymbol{g}_{,\boldsymbol{u}} & \boldsymbol{g}_{,\boldsymbol{\Lambda}} & \boldsymbol{g}_{,\boldsymbol{v}} \\ N^\top_{,\boldsymbol{u}} & N^\top_{,\boldsymbol{\Lambda}} & \boldsymbol{0}_{1\times q} \end{bmatrix}, \tag{7}$$

where j corresponds to the j^{th} increment and the comma notation has been used to denote differentiation.

3 RESULTS

Consider the classical nonlinear finite element benchmark problem of an hinged cylindrical roof, drawn schematically in Figure 1. The radius of the shell is $R = 2540\,\text{mm}$ with hinged longitudinal edges of length $L = 508\,\text{mm}$ and free circumferential edges of equal arc-length $B = 508\,\text{mm}$. The thickness, Young's modulus and Poisson's ratio of the shell are $t = 6.35\,\text{mm}$, $E = 3102.75\,\text{MPa}$ and $\upsilon = 0.3$, respectively. A transverse point load P_c is applied at the centre C of the roof planform.

The shell is discretised into a 31×31 node mesh of 100 fully integrated 16-node, total Lagrangian shell elements using the shell director parametrisation of

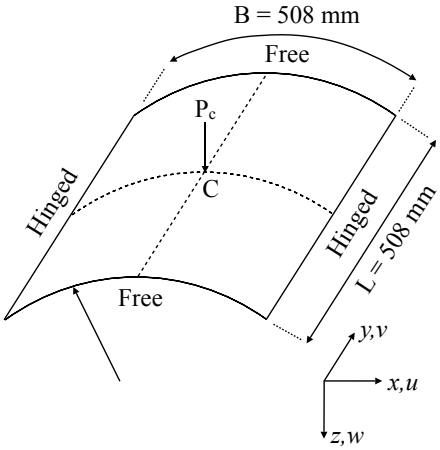

Figure 1: Hinged cylindrical shell with a central point load.

Ramm (Ramm 1977) (two rotations per node, no drilling around director). The effects of shear and membrane locking are minimised by using cubic isoparametric interpolation functions and by refining the mesh sufficiently until convergence with respect to a 68×68 element mesh of reduced integration S4R elements of the commercial finite element software ABAQUS is obtained.

Figure 2 shows a number of equilibrium paths plotted in terms of the transverse displacement w_c versus the applied transverse load P_c at the centre C of the roof. Blue segments denote stable equilibrium paths (all eigenvalues of the tangential stiffness matrix are positive), whereas red segments denote unstable equilibrium solutions (at least one negative eigenvalue). Black points correspond to critical points, *i.e.* equilibrium solutions where at least one eigenvalue of the tangential stiffness matrix is exactly zero. Limit points are always symmetry-preserving bifurcations, *i.e.* no additional branch intersects the curve. At a pitchfork bifurcation point, a symmetry-breaking secondary branch intersects the primary branch.

The equilibrium path beginning at the origin (path 1) in Figure 2 is the typical fundamental path reported in numerous studies in the literature, *e.g.* (Zhou, Stanciulescu, Eason, & Spottswood 2015). In total, there are three secondary bifurcation branches emanating from the fundamental path (paths 2-4), but in an experimental test, these branches can not be realised as they are unstable equilibria under the imposed load control regime. Additional tertiary branches (paths 5-7) emanate from the three secondary branches (paths 2-4), which either connect back to the secondary branches from which they emanated (paths 5 and 6), or connect to other secondary branches. For example, tertiary branch 7 connects branch 4 to branch 3.

As shown in Figure 2, the fundamental path 1 and bifurcation branch 2 traced by ABAQUS' Riks solver using S4R shell elements matches closely with the present model. To trace the bifurcated branch 2 in ABAQUS, an initial imperfection based on a linear eigenvalue analysis needs to be imposed. All other bifurcation branches are much more cumbersome to

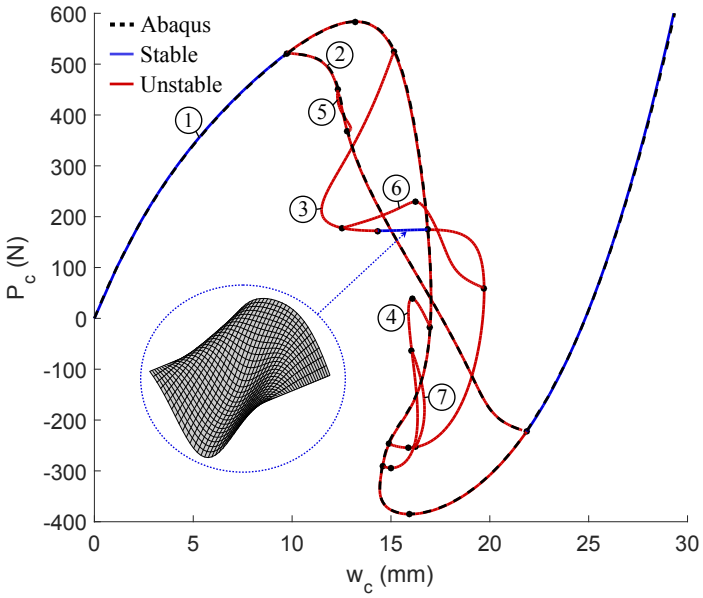

Figure 2: Design space of equilibrium curves of an hinged cylindrical shell with a central point load. The path numbering system is shown in circles. The ABAQUS reference solution is superimposed as a black dashed curve. Path 1 corresponds to the classical fundamental path; paths 2-4 are secondary branches bifurcating from the fundamental path; and paths 5-7 are tertiary branches emanating from the secondary branches.

trace in this manner because linear eigenvalue analysis would need to be performed in the vicinity of each critical point, and the analysis then restarted with the pertinent imperfection.

Interestingly, Figure 2 also shows a localised region of stability on bifurcation branch 3. Identifying this region experimentally is not a trivial task, as this region cannot be reached by simply increasing the applied load from the unloaded state. Rather, a load of around 200 N would be applied, and the roof then perturbed into the mode shape corresponding to the localised region of stability.

It is, however, interesting to investigate how this stable region evolves as individual parameters of the roof are varied. This could be done parametrically by running the full solution shown in Figure 2 for a number of different models. Given that the stable region is bounded by two limit points, a minimum on the left and a maximum on the right, a computationally more efficient method is to use the capabilities of generalised path-following to evaluate the locus of these two critical points – a so-called *foldline*.

One of the black curves in Figure 3 shows this foldline, which was traced with a single call to the generalised path-following algorithm and delimits the boundary of the stable region for changes in shell thickness. The direction of decreasing thickness is indicated by the direction of the arrows with the $-t$ label. Visually, this region is akin to an island of stability with extremities at $t = 7.12$ mm, where the stable region ceases to exist, and the limiting case of zero thickness. On one side, the foldline approaches a locus of pitchfork bifurcation points – herein referred to as a *pitchfork line* – which shows that the bifurcation

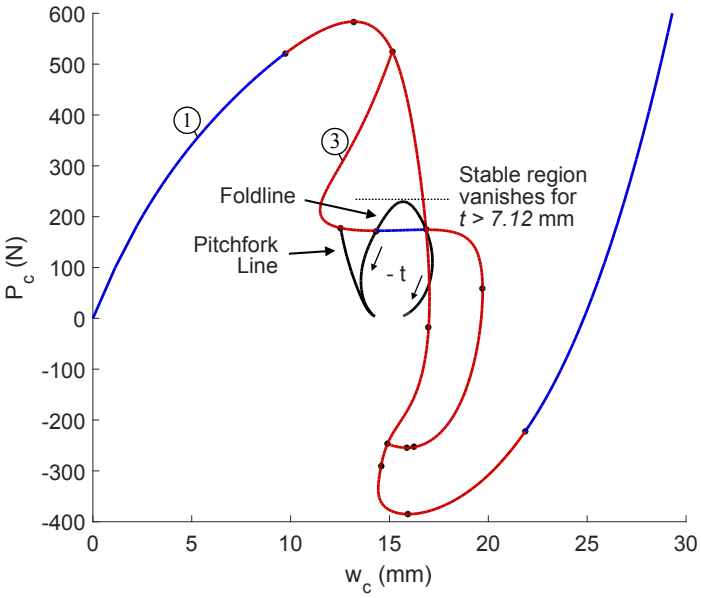

Figure 3: Evolution of the stable region on secondary branch 3 with varying shell thickness (direction of decreasing thickness is shown by the arrows with label $-t$.). A generalised path-following algorithm allows the analyst to trace the locus of limit points that bound the localised stable region.

point and minimum limit point merge as the thickness of the shell decreases. For clarity, the evolution of the stable region is also shown parametrically in Figure 4 where portions of the fundamental path 1 and secondary branch 3 for $t = 4.76\,\text{mm}$ and $t = 3.175\,\text{mm}$ are shown in a three-dimensional plot.

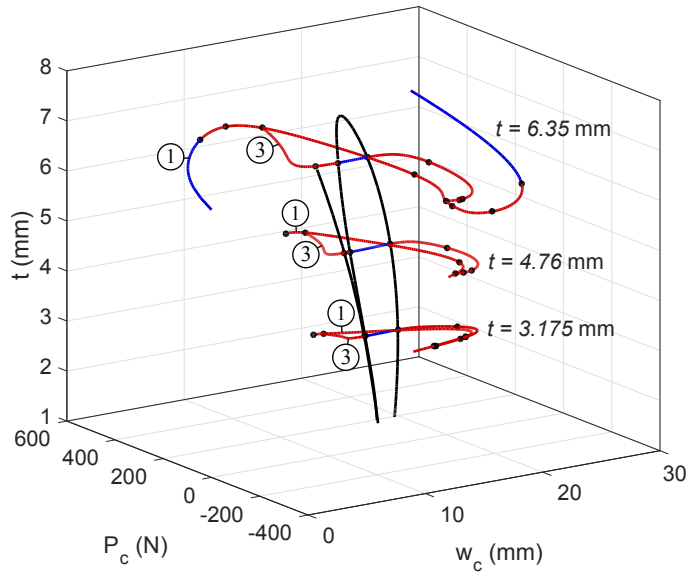

Figure 4: Three-dimensional view of Figure 3 with two superimposed portions of the fundamental path 1 and secondary branch 3 for $t = 4.76\,\text{mm}$ and $t = 3.175\,\text{mm}$.

4 CONCLUSIONS

The capabilities of generalised path-following have been demonstrated by means of a simple benchmark problem – the snap through of a shallow cylindrical roof. For the chosen benchmark shell thickness, a localised region of stable equilibrium exists on one of the unstable equilibrium branches. The evolution of this stable region with changing shell thickness was determined by tracing the locus of the critical limit points that separate the stable and unstable portions of the equilibrium curve. Hence, we established a two-dimensional manifold of stable equilibria in load-displacement-thickness space, which can be graphically interpreted as an *island of stability*.

In conclusion, this simple example has highlighted some of the key features of generalised path-following:

- Limit and pitchfork bifurcation points are evaluated exactly while an equilibrium path is traced.
- Bifurcation branches emanating from another equilibrium path can be systematically explored.
- A locus of limit or pitchfork bifurcation points can be followed without parametrically evaluating the entire equilibrium path.

The implications of these features are that the nonlinear design space of shell structures can be robustly explored in a computationally efficient manner, which is especially valuable for imperfection sensitivity and optimisation studies.

REFERENCES

Eriksson, A. (1997). Equilibrium subsets for multiparametric structural analysis. *Computer Methods in Applied Mechanics and Engineering 140*, 305–327.

Pirrera, A., D. Avitabile, & P. M. Weaver (2012). On the thermally induced bistability of composite cylindrical shells for morphing structures. *International Journal of Solids and Structures 49*, 685–700.

Ramm, E. (1977). A plate/shell element for large deflections and rotations. In *Formulations and Computational Algorithms in Finite Element Analysis*, Cambridge, MA, USA. MIT Press.

Zhou, Y., I. Stanciulescu, T. Eason, & M. Spottswood (2015). Nonlinear elastic buckling and postbuckling analysis of cylindrical panels. *Finite Elements in Analysis and Design 96*, 41–50.